Proceedings of ASME Turbo Expo 2011
GT2011
June 6-10, 2011, Vancouver, British Columbia, Canada

GT2011-45699

EFFECTS OF CONTACT INTERFACE PARAMETERS ON VIBRATION OF TURBINE BLADED DISKS WITH UNDERPLATFORM DAMPERS

C.W. Schwingshackl
Imperial College London
London, UK

E.P. Petrov
Imperial College London
London, UK

D.J.Ewins
Imperial College London
London, UK

ABSTRACT

The design of high cycle fatigue resistant bladed disks requires the ability to predict the expected damping of the structure in order to evaluate the dynamic behaviour and ensure structural integrity. Highly sophisticated software codes are available today for this nonlinear analysis but their correct use requires a good understanding of the correct model generation and the input parameters involved to ensure a reliable prediction of the blade behaviour. The aim of the work described in this paper is to determine the suitability of current modelling approaches and to enhance the quality of the nonlinear modelling of turbine blades with underplatform dampers. This includes an investigation of a choice of the required input parameters, an evaluation of their best use in nonlinear friction analysis, and an assessment of the sensitivity of the response to variations in these parameters. Part of the problem is that the input parameters come with varying degrees of uncertainty, since some are experimentally determined, others are derived from analysis and a final set are often based on estimates from previous experience. In this investigation the model of a commercial turbine bladed disc with an underplatform damper is studied and its first flap, first torsion and first edgewise modes are considered for 6EO and 36EO excitation. The influence of different contact interface meshes on the results is investigated, together with several distributions of the static normal contact loads to enhance the model setup and hence increase accuracy in the response predictions of the blade with an underplatform damper. A parametric analysis is carried out on the friction contact parameters and the correct setup of the nonlinear contact model to determine their influence on the dynamic response and to define the required accuracy of the input parameters.

NOMENCLATURE

α	Angle of a cottage roof damper
μ	Friction coefficient
Ω	Rotational speed
ω	Principal vibration frequency
C	Damping matrix
f	nonlinear friction interface force
F_{exi}	Excitation force
F_{fri}	Friction force
K	Stiffness marix
k_t	Tangential contact stiffness
k_n	Normal contact stiffness
M	Mass matrix
m_D	Damper mass
mj	Number of harmonics
n_{ele}	Number of elements
N_0	Static normal load distribution
p	Excitation force
q	Blade displacement vector
Q_j^{cs}	Harmonic coefficients
r_D	Distance from rot. axis to damper centroid
x_{rel}, z	Relative displacement

INTRODUCTION

The availability of advanced linear finite element codes, in combination with ever increasing computational power, provides highly refined and accurate modelling methods for the development of aircraft engine components. Detailed models allow very accurate predictions of the linear dynamic behaviour of single components which correlate well with measured data. This good correlation can decrease significantly when two previously validated components are combined to form an assembly. Many nonlinear joints are present in a gas turbine engine assembly. Some of them are purpose-built to increase blade damping: such as underplatform or tip dampers, and the others are inherent in the bladed disc design: e.g. in blade roots, seals, flange joints. The nonlinear dynamic effects introduced by the mechanical joint can lead to errors in the response prediction if not included in the analysis. The simulation of the nonlinear dynamic behaviour of these joints requires special computational tools that incorporate the nonlinear effects in the dynamic model and produce a correct representation of the assembled structure.

Significant efforts aimed at developing such tools have been made recently [1]-[6], including those made by the authors at Imperial College London (see Refs.[6]-[12]), resulting in the nonlinear dynamics code, FORSE. Experience with previous nonlinear dynamic simulations has shown that in order to obtain reliable results which correlate well with measured data, a correct setup of the analysis model matters as much as the accuracy of the tool itself. It is important to understand how to setup the nonlinear models and how to select the correct input parameters, which can be provided from measured data [13]-[17], be part of simulation results, or based on previous experience, to ensure a successful simulation of the nonlinear dynamic behaviour.

The aim of the presented work is to evaluate the modelling approach and enhance the quality of the nonlinear model setup for turbine blades with underplatform dampers. It includes a discussion of the required modelling parameters, an evaluation of their best use for a nonlinear friction analysis, and an assessment of the sensitivity of the dynamic response towards variations in the setup parameters.

FORCED RESPONSE ANALYSIS: A SCHEME

The code, FORSE, used here for the parametric analysis is based in the multiharmonic representation for steady-state response and large scale realistic friction interface modelling of bladed discs. Major features of the methodology were described in Refs. [6]-[12] and in this paper only a general scheme of the analysis is overviewed. The equation for vibration of a bladed disc consists of a linear part which is independent on vibration amplitudes and non-linear, friction interfaces and can be written in the following form:

$$\boldsymbol{K}\boldsymbol{q}(t)+\boldsymbol{C}\dot{\boldsymbol{q}}(t)+\boldsymbol{M}\ddot{\boldsymbol{q}}(t)+\boldsymbol{f}(\boldsymbol{q}(t))-\boldsymbol{p}(t)=\boldsymbol{0} \qquad (1)$$

where $\boldsymbol{q}(t)$ is a vector of bladed disc displacements; $\boldsymbol{K}$, $\boldsymbol{C}$ and $\boldsymbol{M}$ are stiffness, damping and mass matrices of its linear model; $\boldsymbol{f}(\boldsymbol{q}(t))$ is a vector of non-linear, friction interface forces, which is dependent on displacements and velocities of the interacting nodes and $\boldsymbol{p}(t)$ is a vector of periodic exciting forces. The variation of the displacements in time is represented by a restricted Fourier series, which can contain as many, *n*, and such harmonic components as it is necessary to approximate the solution searched, i.e.

$$\boldsymbol{q}(t)=\boldsymbol{Q}_0+\sum_{j=1}^{n}\boldsymbol{Q}_j^c\cos m_j\omega t+\boldsymbol{Q}_j^s\sin m_j\omega t \qquad (2)$$

where $\boldsymbol{Q}_j^{c,s}$ are vectors of harmonic coefficients for system DOFs; m_j are numbers of harmonics that are used in the multiharmonic displacement representation; ω is the principal vibration frequency. The flowchart of the calculations performed with the code is presented in Fig. 1. The contact interface elements developed in Ref.[7] are used for modelling of nonlinear interactions at contact interfaces and analytical expressions for the multiharmonic representation of the nonlinear contact forces and stiffnesses.

The forced response analysis requires the appropriate choice of values of major parameters for the contact interface elements and the bladed disc model. These parameters can be separated into three main groups: (i) the friction interface parameters that describe the material properties of the contact area, (ii) the modelling parameters that define the nonlinear model and its excitation, and (iii) the analysis parameters which control the accuracy and speed of the calculation.

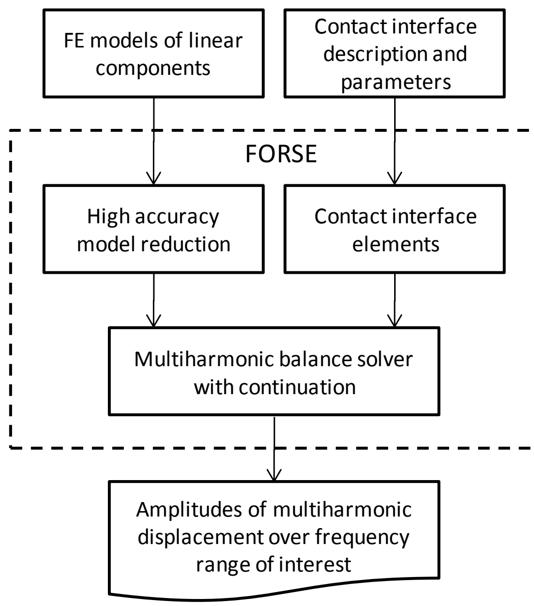

Figure 1 Scheme of the forced response analysis

FRICTION INTERFACE PARAMETERS

The friction contact interface modelling is based on the friction model proposed in [6, 7] which is illustrated in Fig. 2. The friction model uses several input parameters for a computation of the contact interactions. These include the friction coefficient, μ, tangential and normal contact stiffnesses, k_t and k_n, and the static normal load, N_0. Three first parameters in this list characterize the properties of the pairing surfaces and currently are determined experimentally.

Moreover, the friction contact model allows for a variation of the normal load, N_0, including the possibility of separation between the two surfaces and motion along a line in the friction contact plane. A combination of two such elements with alignments in the contact plane along two perpendicular directions is used to model interactions under three dimensional motion: planar motion in the contact plane and the motion along normal direction to the contact plane.

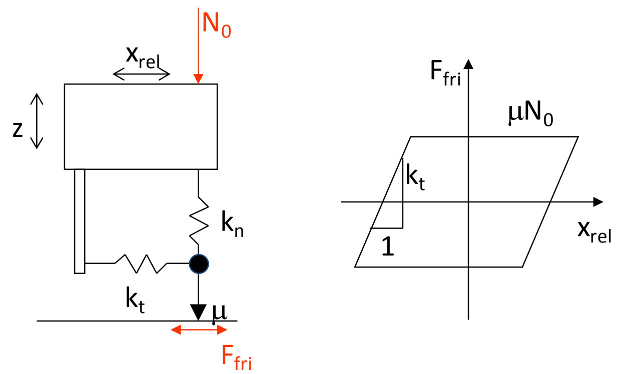

Figure 2 Generic friction model

The friction coefficient can be measured with a friction test rig [13]-[14] under the correct operational conditions, where the hysteresis in Fig. 3 allows an accurate extraction of the correct values. The friction coefficient depends on the material pairing, the contact surface condition, and on the temperature of the contact interface. If no direct measurements are available then an estimate of the friction coefficient should be based on know values under similar conditions. Generally it has been observed that it will drop from 0.6-0.8 for dry contacts at room temperature to 0.2-0.4 at high temperatures with a relatively small uncertainty on a measured value.

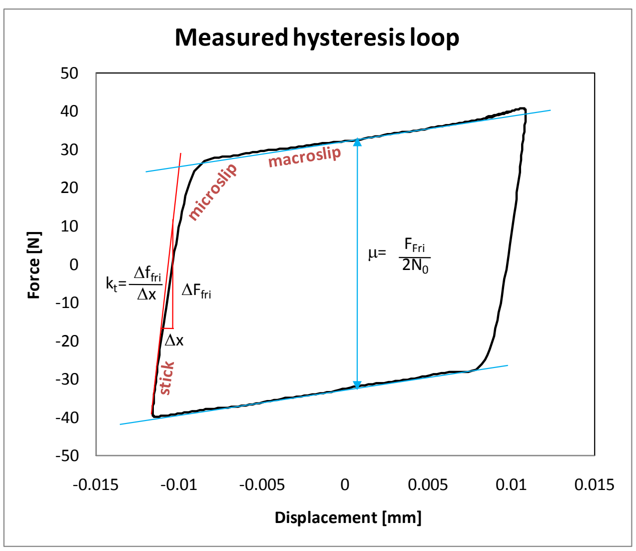

Figure 3 Friction parameter extraction from measured hysteresis loop

The tangential contact stiffness, k_t, describes the elastic deformation of the contact area before slip occurs. It can be extracted from a measured hysteresis loop in Fig. 3 as well and is therefore known for a given set of interface conditions. The material pairing, surface finish and operating temperature play an important role on the extracted stiffness, and the correct values must be used in the analysis. The normal contact stiffness, k_n, contributes to the flexibility of the contact surfaces in the normal direction and the dynamic normal load variation. Although there are attempts to experimentally measure k_n [18], no such measurement data was available for this investigation, and its value was therefore based on previous experience.

ADDITIONAL CONTACT INTERFACE MODELLING PARAMETERS

The modelling parameters for the nonlinear analysis include also the static normal load distribution, N_0, and the number and location of the nonlinear elements on the contact surface, n_{ele}.

Two approaches are currently in use to obtain the static normal load values, N_0, between the contact surfaces. A static finite element analysis or simple equations can be used to calculate the contact load. The FE analysis provides a detailed normal stress distribution over the contact, which can be converted to an static normal load distribution with the help of the known nonlinear element areas [14]. If a finite element solution is not available, then an analytic calculation can yield a normal static load value. The latter approach leads to less accurate results, as a single value will be uniformly distributed over the contact, but in the absence of accurate FE results it can be used in the nonlinear response calculation. The normal static load depends with the power of two on the rotational speed of the structure, since the loading is mostly caused by centrifugal forces. An analysis must therefore be carried out at an appropriate rotational speed to ensure the correct loading.

A further modelling parameter are the contact interface meshes. They discretises the contact areas and their location and density will influence the resulting response. Each element connects two contact nodes, one on each of the contact surfaces, and calculates the resulting relative displacement between the two nodes. It is therefore important that matching or at least close nodes are available on both sides of the model, to ensure good accuracy. The nonlinear mesh must cover the entire contact area and it must be fine enough (n_{ele}) to capture local differences in the contact behaviour, since small slipping areas can introduce significant amounts of damping. It is important to consider the required mesh density and the element distribution with great care to minimise the size of the mesh and to optimise computational time, without losing accuracy in the nonlinear calculation.

A final model parameter is the excitation force. Ideally it will be derived from a CFD analysis, in which case it can be applied as a modal excitation, or if unknown, a harmonic force excitation can be applied to the blade to reach expected displacement levels.

MULTIHARMONIC ANALYSIS PARAMETERS

The analysis parameters control the accuracy and speed of the calculation. The two main values are the number of included modes, and the number of harmonics used which are both provided by the initial linear finite element analysis.

The number of available modes defines how accurately the local deformations of the contact can be reproduced, and therefore significantly influences the contact conditions. Hitherto, quite a large number of modes were required to achieve convergence, but a new accurate method has recently become available [11] which drastically reduces the required number of modes. The new method does not rely solely on modes to calculate the local deformations, but also includes the static flexibility of the contact area. Since the presented study was carried out before this new method became available, the number of modes remained an important input factor.

The nonlinear response calculation is based on a multiharmonic expansion to increase the accuracy of the results, and therefore enough harmonics should be used to take full advantage of the method.

The discussed input parameters can have a significant effect on the calculation time and it is, therefore, very important to evaluate the possible gain in accuracy against the sometimes significant increase in computational expense.

To increase this understanding and improve the current setup approach, a parametric analysis has been carried out for a turbine bladed disk with an underplatform damper.

GENERAL SCHEME OF THE PARAMETRIC STUDY

Based on previous experience with nonlinear friction models, a nominal nonlinear model of a turbine blade with an underplatform damper was created and a parametric study of the 6 and 36 engine orders (EO) carried out. This nominal model uses measurement data for the setup, where available, otherwise it is based on simulated and calculated values, and an experience-based estimation of parameters. The nominal model represented a typical state-of-the-art setup which would have most likely been used for such a type of analysis at the time of the investigation. A variation was then applied to each of these parameters to investigate their influence on the nonlinear dynamic response and to improve the future setup of the nonlinear models.

A finite element sector model was used for a bladed disc comprising 66 blades. The sector model contains approximately 720,000 DOFs (see Fig. 4(a)). The sector model FE mesh at its contact interface with the damper consisted of relatively coarse triangular elements, which could not be easily modified. The modal model of the bladed disc sector model was calculated using in-house FE solver. The model includes natural frequencies and mode shapes for first 48 modes of the bladed disc sector determined for each of the EO analysed.

A schematic underplatform damper in Fig. 4(b) indicates the five contact zones on each side that are in contact with the blade. While creating a finite element mesh for the damper great care was taken to ensure that a fine mesh at the contact surface was created, to provide enough nodes in the vicinity of the blade contact nodes. This led to a mesh with approximately 50,000 DOFs. A modal analysis with 256 modes was carried out to capture localised deformations of the contact surface.

The blade and damper models were available in different files, which made a static normal load calculation with a finite element program quite difficult, and it was therefore decided to use an analytical formula obtained in reference [12] to calculate the static normal load of the damper, N_0.

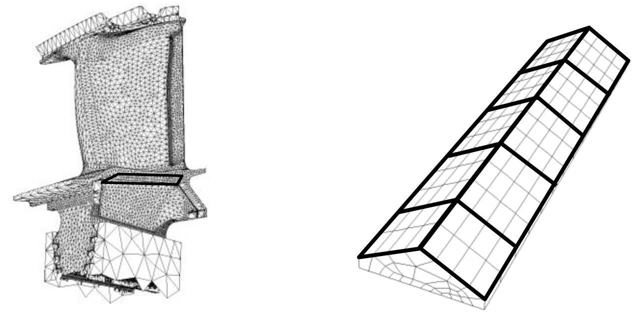
a) b)

Figure 4 The investigated turbine blade (a) and a schematic underplatform damper (b) with ten contact zones

$$N_1 = N_2 = \frac{m_D r_D}{2(\cos\alpha + \mu\sin\alpha)}\Omega^2 \tag{3}$$

Equation 3 takes account of the rotational speed of the engine, Ω, the inclination of the contact surfaces, α, the damper mass, m_D, the distance from the rotation axis, r_D, and the influence of friction coefficient, μ, to provide a static normal load that can be uniformly distributed over the entire contact surfaces.

The nominal friction coefficient, μ=0.3, and the tangential contact stiffness, k_t=5e4N/mm^3 were based on previously measured values at high temperatures and presented the starting point for the parameter variation. In absence of a measured normal contact stiffness, k_n, it was assumed to be identical to the tangential contact stiffness, k_t.

A set of ten contact interface elements were used as a starting point for the investigation with a single nonlinear friction contact element placed in the centre of each contact patch of the damper. This configuration can be seen in Fig. 5 together with a set of additional meshes that were also investigated during the parameter study.

The nominal model includes 48 modes for 6 and 36 EO families of bladed disc modes, and 48 modes of the damper model. During the parameter analysis the blade modes were kept constant, whereas the number of damper modes was varied, to study their influence on the results.

Since no CFD data was available for the present analysis a harmonic excitation, based on previous experience values, is assumed and applied to the leading edge tip, to reach expected displacement amplitudes.

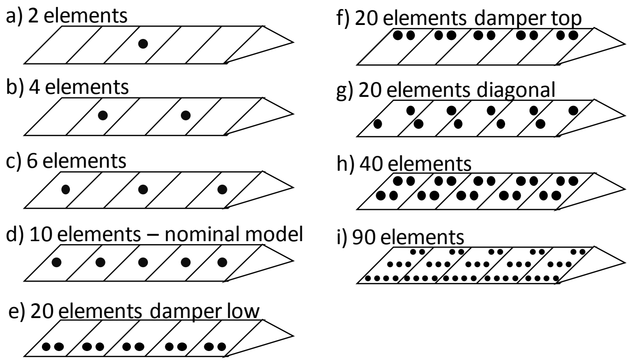

Figure 5 Investigated mesh configurations

Based on the nominal model, each input contact interface parameter underwent approximately ±100% variation to investigate its influence on the amplitude and frequency response of the 1st flap (1F), 1st torsion (1T), and 1st edgewise (1E) modes of the 6 and 36 engine order response. Additional nonlinear model configurations were also investigated, including different mesh sizes with 2 to 90 elements (see Fig. 5), varying element locations and changes in the normal load distribution along the damper.

Nine harmonics were kept in the nonlinear analysis of the bladed disc.

SUMMARY OF 36 EO RESULTS

The variation of the input parameters from their nominal values for two engine orders and the 1F, 1T and 1E modes led to a large amount of data. To make this data more accessible, the discussion will focus on the results obtained for the 36 EO, since both engine orders showed rather similar behaviour. Significant differences between the 6EO and 36EO case, where they appear, will be discussed as well. An initial discussion of these summarised results will be followed by a more detailed discussion of the 1F mode.

A summary of the response amplitude data for the 36EO case can be found in Fig. 6 and for the natural frequencies in Fig. 7. These plots show the behaviour of the three investigated modes for five input parameters. The plots represent the calculated range of amplitude and frequency caused by a variation of each input parameter. Here, the nominal values are represented by 0%, a reduction is indicated by a negative value, and an increase by a positive percentage. The parameters investigated were varied over approximately a ±100% range, which especially in the case of the measured parameters, represented variations that where larger than expected. The results in Fig. 6 and Fig. 7 show that the first torsion (1T) mode is the most sensitive with regards to the amplitude and the first edgewise (1E) with regards to frequency. Several of the parameters caused similar variations, highlighting their equal importance for the nonlinear friction interface analysis of a turbine blade with an underplatform damper.

The influence of the combined tangential and normal contact stiffnesses, k_t and k_n, on the amplitude of the turbine blade with an underplatform damper varies significantly between the three investigated modes, leading to amplitude changes of more than 200% for the 1T mode and less than 60% for the 1E mode. A lower contact stiffness value leads to higher amplitudes, since it allows for additional elastic deformation before the damper starts to slip. The influence of the contact stiffness on the frequency response in Fig. 7 is 10% or less, which represents an average value of the calculated variations. A similar behaviour range was detected for the 6EO case, with the main difference being that the 1F mode was the most sensitive. This indicates a correlation between the contact stiffness and the excitation order, and highlights the fact that an acceptable model for one condition may not be satisfactory for another. The sensitivity of all modes towards the contact stiffness highlights the need for an accurate input value, which ideally should be determined experimentally for the given contact condition, or selected very carefully from previous results.

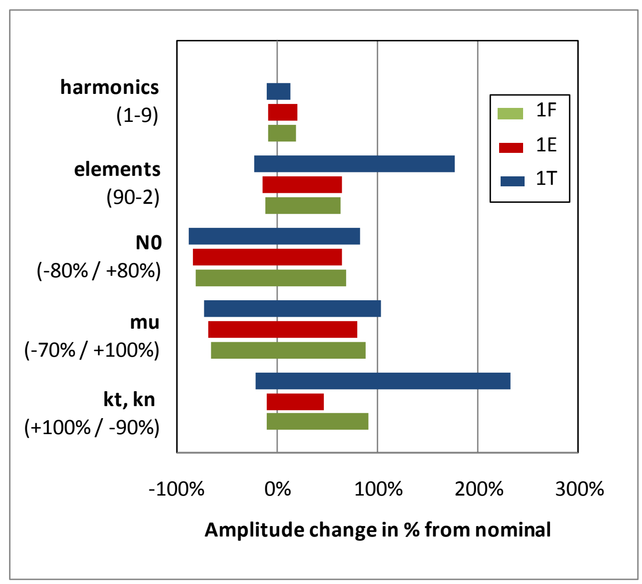

Figure 6 36EO – Amplitude variation in % from the nominal model for various parameter changes

The friction coefficient, μ, shows a strong influence on the amplitudes of all the investigated modes in Fig. 6. The friction coefficient determines whether the damper is continuously slipping with very low levels of energy dissipation (small μ), of if it is stuck in which case it just couples the blades but does not dissipate any energy (large μ), or if it operates in a range where it efficiently dissipates energy. The investigated -70/+100% variations of the friction coefficient did cover a large part of the operational range of the damper, which is mirrored by its strong influence on the amplitude results. A shift from lightly damped to stuck conditions, due to the change in the friction coefficient, also influences the resulting response frequency. A significant reduction in the friction coefficient, μ, nearly uncouples the blades, leading to a lower resonance frequency whereas in the case of a stuck damper it couples the two blades with the tangential contact stiffness, k_t, leading to higher resonance frequencies. It is important to have an accurate knowledge of the correct friction coefficient for an analysis, since its influence on the response of the turbine blade with an underplatform damper is strong.

The static normal loads N_0, have been calculated analytically with Equation 3 and applied uniformly over the contact areas. Since the friction force, F_{fri}, linearly depends on the friction coefficient, μ, and the normal load, N_0, the very similar behaviour of the amplitude in Fig. 6 is not surprising. Small static normal loads, N_0, will not introduce enough pressure in the contact area to dissipate any significant amount of energy, leading to large amplitudes. An increase in N_0 causes the elements to slip properly, introducing more friction damping and, in turn, smaller peak response amplitudes. With a further rise in N_0, fewer elements will be slipping, leading to a reduction in friction damping, and an increase in peak response amplitude. At very high N_0 values, the contact gets stuck and transmits force via the tangential contact stiffness, k_t, only. The influence on the response frequency in Fig. 7 is rather less prominent, since a 80% reduction in the normal load was not enough to fully uncouple the two blades, leaving some of the contact stiffness influence in place.

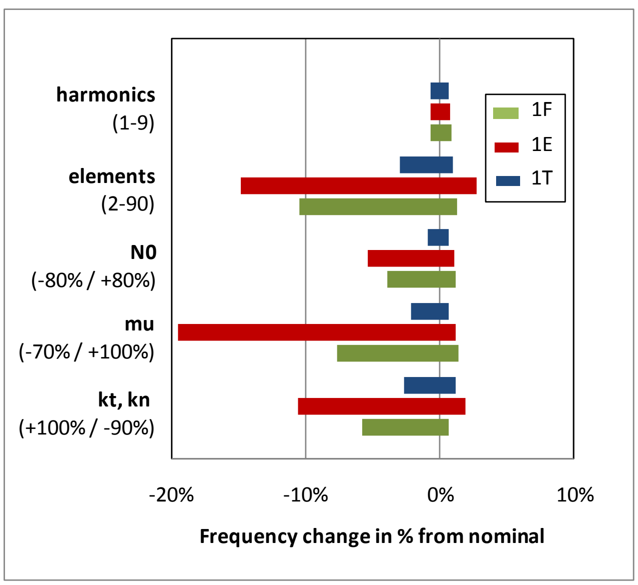

Figure 7 36EO – Frequency variation in % for various parameter changes

The variation of the mesh density, from one element on each side of the damper to 90 elements spread evenly over the contact patches (see Fig. 5) shows that very coarse meshes can lead to over-predictions of the amplitudes (see Fig. 6), and quite significant lower resonance frequencies (see Fig. 7). This is due to the fact that in the case of the smaller number of the elements only a few, possibly localised, displacements can affect the contact interaction forces, whereas in the case of the larger number of elements the influence of the entire surface is captures. For a very rough mesh all contact elements may be slipping, but if they are not located at nodes with large amplitudes, then the total energy dissipation can be smaller than in reality. A fine mesh is more likely to capture maximum displacement locations and therefore to calculate the dissipated energy more accurately and the stiffness of the nonlinear contact interface. As a result the mesh variation can generally affect resonance frequency and amplitude values.

This highlights the need for an adequate number of elements in the model to capture all the local stick-slip-separation events in the contact. In particular, the 1T mode, with strong differences in relative displacement along the damper axis, requires a fine mesh to capture the proper dynamic behaviour. It was observed, that the 6EO case requires a finer mesh than the 36EO case to ensure convergence. When meshing a nonlinear contact interface it is therefore recommended that a convergence check is carried out to minimise the influence of discretisation errors.

The final parameter in Fig. 6 and Fig. 7 is the required number of harmonics. Results for 1 to 9 included harmonics have been calculated. For the investigated case, the amplitude and frequency variations due to the number of harmonics are significantly smaller than the influence of all the other investigated parameters, and two odd harmonics lead to near convergence of the response. An increase in included harmonics quite significantly increases the calculation time and a relatively low number of harmonics can therefore be used.

SOME MORE DETAILED RESULTS

The summary in the previous section shows the importance of the different input parameters for a correct setup of the nonlinear friction analysis, without going into much detail of the results. Some of the results will now be discussed in more detail to provide a better understanding, and to highlight some further considerations for setting up a nonlinear friction contact analysis.

Fig. 8 shows the responses for the 36EO 1F mode response with a combined variation of k_t=k_n over a range from -99% / +900%. The blade response without a damper and with a stuck damper has also been included since these represent the two limiting cases. The frequency transition from a response close to the un-coupled system for low stiffness values to a response close to the locked system for very high stiffnesses can be clearly observed, along with a reduction in the amplitude due to increased slip in the system.

Each resonance amplitude value in Fig. 8 was extracted and added to Fig. 9 together with some values for the 6EO, which shows the dependence of the amplitude on the values of contact interface parameters. The selected range of change for the stiffness parameters was quite large, and especially the lower levels are not usually extracted from tests. Higher levels on the other hand led to converged results. A drop of amplitude for ±100% change in the stiffness values k_t and k_n, is opposed by a nearly linear increase of the amplitude due to the friction

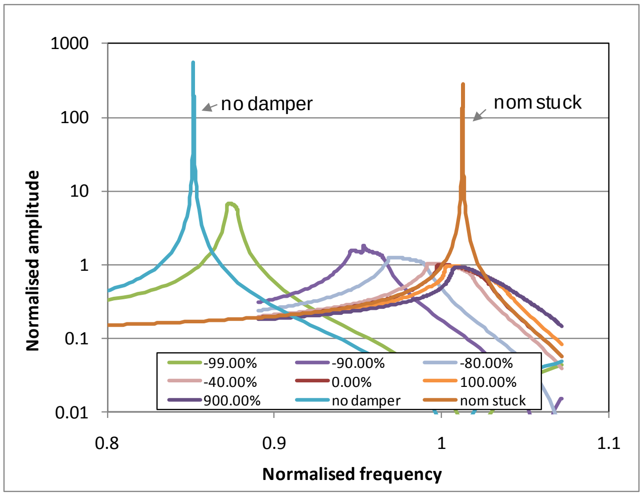

Figure 8 36EO – 1F: Amplitude response for kt=kn variation

coefficient, μ, and the normal load, N_0. It should be noted that a different amplitude behaviour can be expected for stronger variations, with lower friction coefficient and static normal load values starting to increase the amplitude again (this can be seen for the friction coefficient), due to less and less dissipated energy, and higher values leading to a constant amplitude caused by a totally locked contact. Only a small influence of the number of included harmonics can be seen in Fig. 9, where an initial variation of 10% disappears for three or more included harmonics. As previously mentioned, both investigated engine order modes exhibit a relatively similar behaviour, with the 6EO showing a slightly larger sensitivity towards the tangential and normal contact stiffness. During the investigation a large set of these plots was generated for all investigated modes and excitations, which were then summarised to Fig. 6 and Fig. 7.

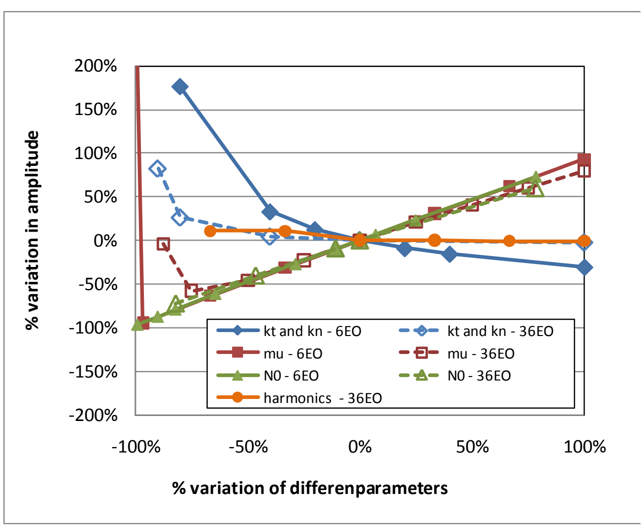

Figure 9 6 and 36EO – 1F: % Variation of amplitude from nominal for different parameters, k_t and k_n, μ, N_0 and m_j

Special consideration was given to the influence of the nonlinear mesh, since initial results indicated a strong dependence. Fig. 10 shows the changes of amplitude for different mesh sizes in more detail for the 6 and 36 EO. At least 10 elements, corresponding to a single element for each contact patch, are required to capture the dynamic behaviour of the damper for 36 EO correctly. In the case of 6EO at least 20 diagonal elements are necessary to achieve convergence. Enough nonlinear elements in the correct positions on the contact must be used to capture all the local forces and moments between the damper and the blade root. A model that may be good enough for one mode may have to be modified for another.

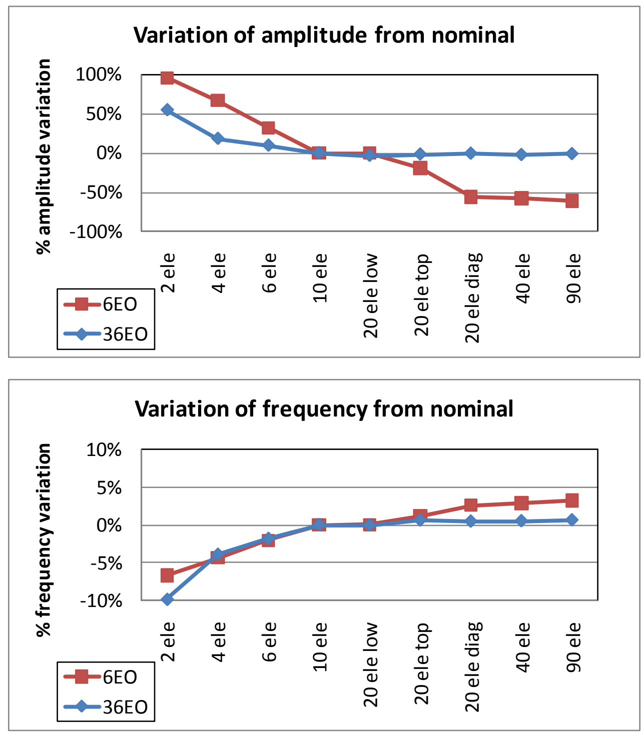

Figure 10 6 and 36EO – 1F: % Variation of amplitude and frequency from nominal for different number of elements

The difference between the three 20 node element configurations in Fig. 10 suggests dependence not only on the number of elements, but also on their locations. This is likely due to the fact that in the previous cases all elements were located along a line on the damper, allowing for a certain amount of relative rotation between the blade and the damper. The 20 diagonal element case prevents this type of motion, leading to a stiffer constraint, and consequently to a lower amplitude and increase in frequency. To investigate this in more detail, the relatively coarse 6-element mesh was modified to provide different element patterns. The generated element distributions can be seen in Fig. 11(b), where the original central distribution was modified to include an off centre symmetric and a random mesh pattern. The resulting amplitudes in Fig. 11(a) change by 25%, indicating a high sensitivity of the coarse mesh towards the element location. The frequency changes were relatively small, with a maximum increase of 1%. Therefore not only the number of elements must be considered when meshing a nonlinear model, but also the location of these elements to ensure that all important forces and torsion moments can be picked up by the analysis. Applying a fine mesh to the damper can eliminate these issues, but it comes at a higher computational cost.

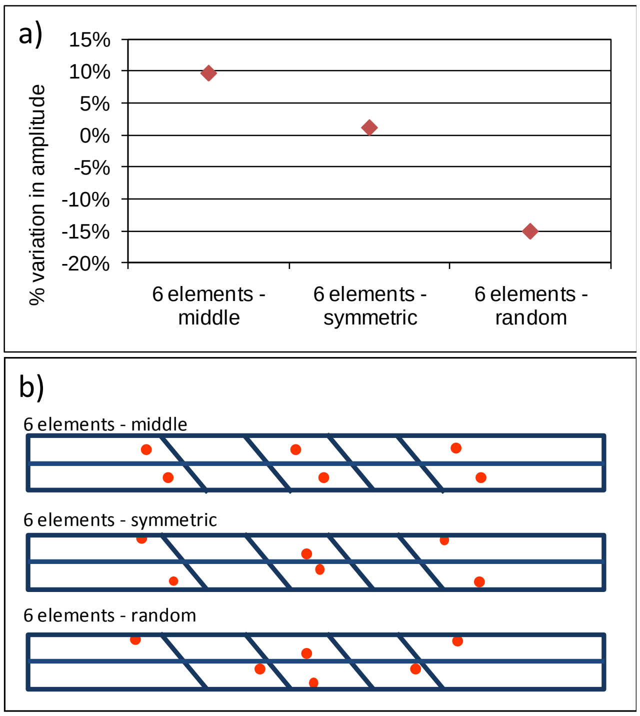

Figure 11 36EO – 1F: (a) Influence of element location on results and (b) the location of the nodes

A non uniform normal load will increase the importance of the number of elements and location even more, since a different location of an element may lead to significantly lower or higher normal load, resulting in different slip-stick conditions. For the present a simple variation of the uniform distribution was applied to the nominal model to investigate its effects on the resulting amplitudes. Starting from the nominal case two modified normal load distributions were created; one with a higher load and one with a lower load in the centre of the damper (see Fig. 12(b)). The total transmitted normal load was thereby kept constant. A load peak in the middle of the damper, with two elements showing very low loads, leads to 20% lower amplitudes than the nominal mode (see Fig. 12(a)), since the low-load elements slip earlier and dissipate more energy. Higher loads at the ends of the damper, with a single element having lower loads in the centre, increase the amplitudes slightly, since the high-load elements will remain stuck longer. The two investigated pressure distributions were randomly generated and do not present a real contact condition, but the

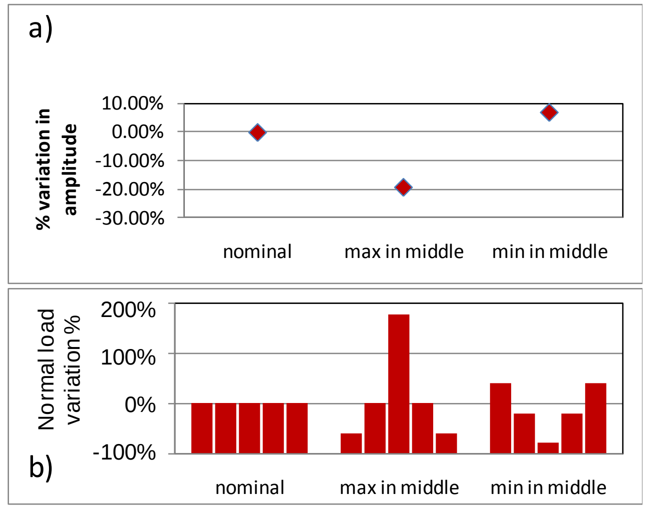

Figure 12 6EO – 1F: (a) Influence of normal load distribution on amplitude and (b) the different distributions

results highlight the influence of the static normal load distribution, on the response and strongly suggest the use of an accurate normal load distribution from a finite element analysis in combination with at fine mesh, instead of a uniformly distributed analytic solution.

In the absence of a measured value for the normal contact stiffness, k_n, this was set equal to the tangential contact stiffness, k_t. To investigate the validity of this approach, the influence of each of these two stiffnesses was calculated separately (see Fig. 13). The tangential contact stiffness, k_t, shows a much larger influence on the resulting amplitudes than the normal stiffness, k_n, especially for low values and the amplitude change of the combined stiffness variation is not much different than the k_t variation on its own. In absence of a known normal contact stiffness, it is therefore an acceptable, also not ideal, approach to set it equal to the tangential contact stiffness, k_t, since the introduced error is relatively small,

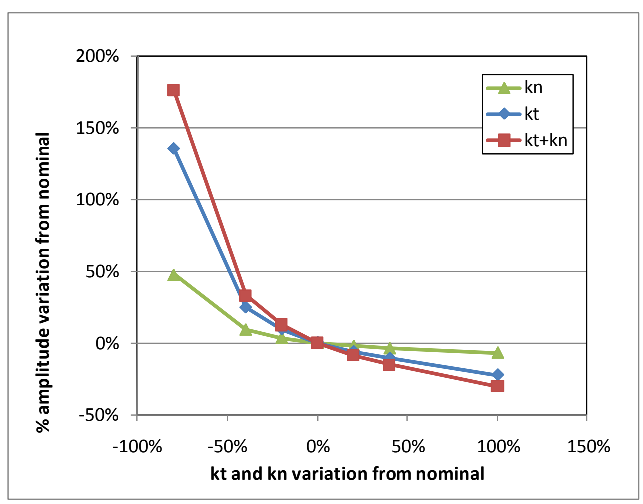

Figure 13 6EO – 1F: influence of tangential and normal contact stiffness on amplitude response

especially for the experienced experimental uncertainty which normally stays within 10%.

The version of the nonlinear code used here represents the flexibility of the contact surfaces purely by its localised mode shapes, which makes the number of included modes an important input parameter. Fig. 14 shows the change in amplitude due to the inclusion of different numbers of damper modes, starting from only 6 rigid body modes up to 256. The first case represents a rigid damper with no flexibility, whereas in consecutive cases more and more flexibility will be taken into account. It can be seen, that although, convergence is observed when a large number of modes is included in the analysis (more than 100), the effect of the number of modes in this particular case is not significant and for all practical purposes 48 modes used for the nominal model are more than sufficient, and even a rigid damper would be acceptable. It should be mentioned here that in other configurations the influence of the number of modes was more important [10] and that a certain amount of flexibility should therefore always be included in the analysis.

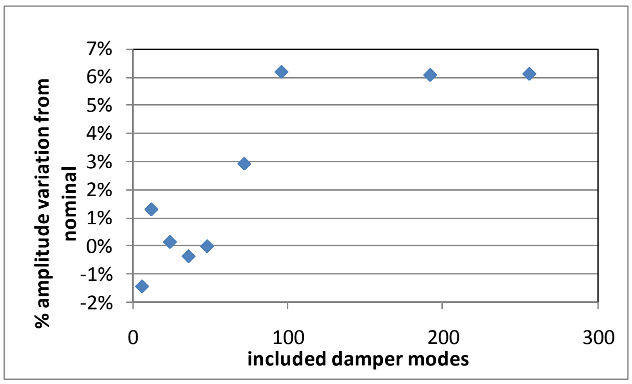

Figure 14 Influence of included modes on amplitude: 1F/36EO

DISCUSSION

The following discussion on the choice of the modelling parameters is based on a parametric study for a turbine blade with an underplatform damper, and it may not be directly applicable to other friction contact interface problems.

The initial linear FE analysis must provide sufficient and accurate modal data to represent not only the global, but also the local deformations in the contact. For the investigated cases two included odd harmonics for the expansion of the displacement variation in time are adequate as the parameter analysis showed that their influence was relatively small. The finite element meshes on the contact surface should be evenly distributed and fine enough to allow the application of a contact interface mesh. Matching element nodes on both contact sides are advisable, but at least close nodes should be provided by the FE model. A nonlinear calculation method that is purely based on modal data requires many modes to achieve convergence, also the resulting error is relatively small, but the use of the approach in reference [11] is advisable to increase the accuracy of the results.

The tangential contact stiffness, k_t, and the friction coefficient, μ, both have a strong influence on the resulting nonlinear amplitudes and resonance frequencies. They represent material properties of the contact and should be based on measured data. The unknown normal contact stiffness, k_n, shows less influence on the results, and an assumed value, similar to the tangential contact stiffness, k_t, is therefore an acceptable, also not ideal solution.

The absolute value of the static normal load and its distribution has a significant influence on the resulting response of the nonlinear structure. Since analytic solutions can only provide the first, but give no indication about the latter, it is much more advisable to use finite element results, to obtain an accurate representation of the contact condition.

The density of the nonlinear mesh and the placement of the elements should be made with great care. The mesh can reflect the static load distribution in the contact, and be able to pick up the dynamic forces and moments that occur during the nonlinear dynamic analysis. A mesh convergence check is highly recommended to minimise the discretisation errors.

The parameter analysis of the turbine blade with an underplatform damper showed that a careful approach to the model setup is required and that some of the parameters have to be applied with great care.

CONCLUSION

To obtain an accurate prediction of nonlinear contact behaviour, not only advanced computational tools are required, but also their correct and effective use must be ensured. For this purpose, a general discussion of the required input parameters for a nonlinear friction interface analysis has been presented, followed by a parametric study for a turbine blade with an underplatform damper. It focuses on the three required input parameter groups, concerning (i) the friction contact interface, (ii) the nonlinear model setup, and (iii) the analysis parameters. Changes to some of the input parameters lead to significant changes in the maximum response amplitude. Their combined influence on the corresponding resonance frequencies was smaller.

The tangential contact stiffness, k_t, the friction coefficient, μ, the static normal load distribution, N_0, and the nonlinear mesh density and distribution, were identified as the most important parameters for a setup of a nonlinear friction interface analysis of a turbine bladed disc with underplatform damper considered here. Accurately measured values should be used as input parameters where available, convergence checks should be carried out for the mesh and the analysis parameters, and detailed simulation data should be used as input data instead of simple analytic solutions.

ACKNOWLEDGMENTS

The authors are grateful to Rolls-Royce Plc. for providing the financial support for this project and for giving permission to publish this work. Special thanks goes to Dr. H. Kurt-Elli and Dr. J. Green of Rolls-Royce for their useful comments on the work.

References

[1] Poudou, O., Pierre, C., 2003, "Hybrid frequency-time domain methods for the analysis of complex structural systems with friction damping", AIAA/ASME/ASCE/AHS/ASC Struct. Dyn. & Materials Conf. Norfolk, USA, Vol. 1, pp. 111-124.

[2] Charleux, D., Gibert, C., Thouverez, F., and Dupeux, J., 2006, "Numerical and Experimental Study of Friction Damping in Blade Attachments of Rotating Bladed Disks", International Journal of Rotating Machinery, Article ID 71302, Pages 1–13.

[3] Chen, J.J., and Menq, C.H. , 2001, "Prediction of Periodic Response of Blades Having 3D Nonlinear Shroud Constraints," ASME Journal of Engineering for Gas Turbines and Power, Vol. 123, pp. 901-909.

[4] Firrone, C.M., Zucca, S., and Gola, M., 2009, "Effect of static/dynamic coupling on the forced response of turbine bladed disks with underplatform dampers", Proc. of ASME Turbo Expo, June 8-12, Orlando, Florida, USA, GT2009-59905.

[5] Cigeroglu, E., An, N., and Menq, C.H., 2007, "Wedge damper modelling and forced response prediction of frictionally constrained blades", Proc. of ASME Turbo Expo, May 14–17, Montreal, Canada, GT2007-27963.

[6] Petrov E.P., and Ewins D.J., 2004, "Generic friction models for time-domain vibration analysis of bladed disks", Transactions of the ASME. J. of Turbomachinery, v 126, n 1, pp. 184-92.

[7] Petrov, E.P., and Ewins, D.J., 2002, "Analytical formulation of friction interface elements for analysis of nonlinear multiharmonic vibrations of bladed discs", ASME J. of Turbomachinery, Vol.125, April, pp.364-371.

[8] Petrov, E.P., 2004, "A method for use of cyclic symmetry properties in analysis of nonlinear multiharmonic vibrations of bladed discs," Trans. ASME: J. of Turbomachinery, Vol.126, January, pp.175-183.

[9] Petrov, E.P. and Ewins, D.J., 2004, "State-of-the-art dynamic analysis for nonlinear gas turbine structures" J. of Aerospace Engineering, Proc. of the IMechE, Part G, vol.218, No G3, pp.199-211.

[10] Petrov, E.P., 2008, "Explicit finite element models of friction dampers in forced response analysis of bladed disks", Journal of Engineering for Gas Turbines and Power, Vol. 130, n 2, pp 022502

[11] Petrov, E.P., "A high-accuracy model reduction for analysis of nonlinear vibrations in structures with contact interfaces", Proceedings of ASME Turbo Expo 2010, GT2010-23295,Glasgow, UK, 2010.

[12] Petrov, E.P., and Ewins, D.J., 2007, "Advanced modelling of underplatform friction dampers for analysis of bladed disk vibration", Journal of Turbomachinery, vol 129, nr 1, pp 143-150.

[13] Stanbridge, A.B., Ewins, D.J., Sanliturk, K.Y., and Ferreira, J.V., 2001, "Experimental investigation of dry friction damping and cubic stiffness non-linearity", Proceedings of the 2001 ASME Design Engineering Technical Conference, Pittsburgh, PA, pp. 2141-2148.

[14] Schwingshackl, C.W., Petrov, E.P., and Ewins, D.J., 2010, "Validation of test rig measurement and prediction tools for friction interface modelling", Proceedings of ASME Turbo Expo 2010, GT2010-23274, Glasgow, UK, 2010.

[15] Filippi, S., Rodrigues, E.B. and Gola, M., 2006, "Experimental characterization of contact hysteresis at high temperatures", Proceedings of the ASME Turbo Expo 2006, Barcelona, Spain, pp 893-902.

[16] Koh, K.-H., and Griffin, J. H., 2007, "Dynamic Behaviour of Spherical Friction Dampers and Its Implication to Damper Contact Stiffness," Journal of Engineering for Gas Turbines and Power, APRIL 2007, Vol. 129, pp.511 – 521.

[17] Gaul, L. and Lenz, J., 1997, "Nonlinear dynamics of structures assembled by bolted joints", Acta Mechanica, vol 125, n 1-4, pp 169-181.

[18] Gonzalez-Valadez, M. , Baltazar, A., and Dwyer-Joyce, R.S, 2010, "Study of interfacial stiffness ratio of a rough surface in contact using a spring model", Wear, Vol. 268, n 2-3, pp 373-379.

